

INTEGRATED LCL FILTERS USED IN GRID-TIED PHOTOVOLTAIC POWER SYSTEMS FOR CONDUCTED EMI REDUCTION

Vuttipon Tarateeraseth

Department of Electrical Engineering, Srinakharinwirot University, Nakhonnayok, Thailand
vuttipon@g.swu.ac.th

Abstract: In this paper, the integration technique of magnetic components of a LCL filter used in grid-tied photovoltaic (PV) power systems for conducted electromagnetic interference (EMI) reduction, especially common-mode (CM) emission, is proposed. Two CM chokes of a LCL filter are integrated into single unit by using an UIU magnetic core. The winding configuration and approximation of differential-mode (DM) and CM inductances of proposed technique are also presented. The DM and CM EMI reduction performances of grid-tied PV power systems without any filter inserted, with conventional separated CM chokes, and with proposed integrated CM choke are evaluated and compared. From the experimental results, it can be concluded that the proposed integrated LCL filter is not only having high EMI attenuation rate comparing to a conventional LCL filter, but also can reduce total physical size, weight, and production cost of grid-tied PV systems.

Keywords: Electromagnetic Compatibility; Electromagnetic Interference; EMI filter; LCL filter; Grid-tied Inverters.

1. Introduction.

In 21st century, with the evaluation of semiconductor devices, power converters and IT technology, modern power electronics are impact not only to conventional energy systems, but also renewable energy systems as well [1-2]. For the renewable energy systems, nowadays, it is well-known that the need for clean power generation is unavoidable because of the global warming and climate change problems. Among all clean power generation technologies, one of the leading potential renewable energy sources of electricity generation is the solar photovoltaic (PV) which is connected to the grid utility by being use of modern power electronic converters [3-4]. Even though, the use of modern power electronics technology gains significant advantages such as the most efficient power conversion with compact physical dimension, the semiconductor devices must be operated at very fast-switching frequency which is the one of the major root causes of electromagnetic interference (EMI) [5]. It is generally known that the malfunction or failure of the performance of electrical/electronic devices, equipments, or systems is probably caused by the high-frequency noises or EMI. Some of EMI issues caused by DC cabling, common-mode disturbances,

and grounding problems in high-power grid-tied PV plants are investigated in [6].

In order to prevent EMI problems and to meet EMI standards, EMI filters are normally placed between the grid-tied PV power systems and the grid utility to limit the EMI noises injecting to the grid utility. Conventionally, for grid-tied PV power systems, LCL or LLCL filters are normally used as a topology of an EMI filter [7]. Moreover, an EMI filter also normally uses discrete components and is composed of a differential-mode choke (DM choke), a common-mode choke (CM choke), X-capacitors, and Y-capacitors [8]. However, by being use of an EMI filter, the total physical dimension, weight, and production cost of grid-tied PV power systems are increased dramatically where the most expensive, weightiest and bulkiest parts of an EMI filter are magnetic components e.g. CM and DM inductors, respectively [9].

Many researches have been proposing various techniques to integrate all EMI filter components using planar PCB with advanced magnetic technology [10-11]. However, in a commercial EMI filter, the use of traditional discrete components and discrete ferrite cores is still the most preferable because it is widespread available and cost-competitive [12]. Moreover, in [13], the technique to integrate CM chokes and Y-capacitors using flexible multilayer foils is proposed. Although, it can reduce total volume up to about 45%, the achieved CM inductance and Y-capacitance are quite low and limited because the proposed structure limits the number of turns that causes the difficulty to design an EMI filter optimally. Therefore, to reduce total physical size, weight, and production cost of grid-tied PV power systems but still use the conventional discrete ferrite cores and components, the technique to integrate two CM chokes used in LCL filters for grid-tied PV power systems into one single unit is proposed in this paper.

2. Basic Operation of a Common-mode Choke

As shown in Fig. 1, a common-mode (CM) choke is connected between line and neutral wires where it is normally used to limit the CM currents.

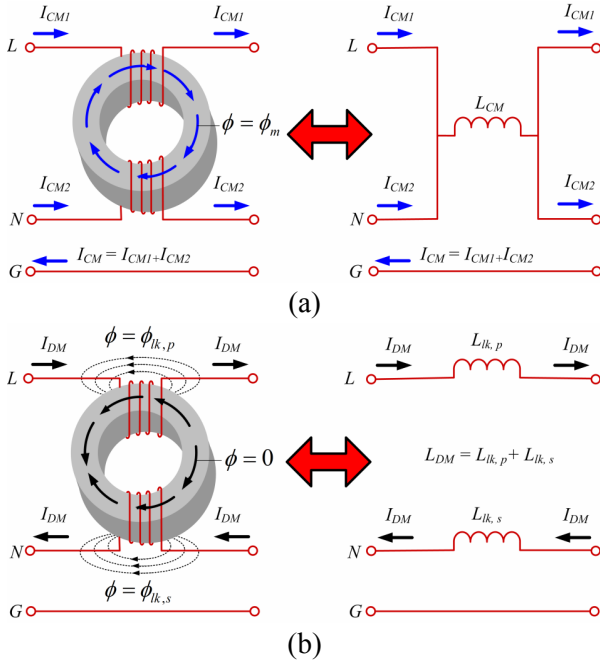


Fig. 1. Operation of a CM choke under: (a) CM current; (b) DM current.

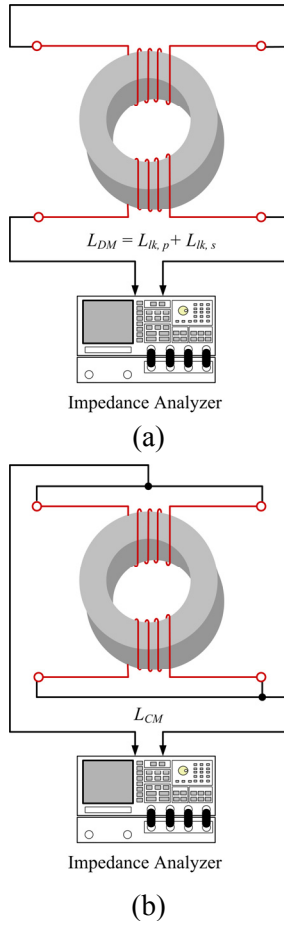


Fig. 2. CM choke measurements: (a) DM inductance measurement; (b) CM inductance measurement.

Generally, for the winding arrangement of a CM choke, two windings with equal number of turns are wound in the same winding direction on the opposite sides of a single ferrite core. The basic operation of a CM choke as CM and DM currents passing through it is shown in Figs. 1 (a)-(b), respectively. It can be seen that the mutual flux is added up with the CM current direction. As a result, a large amount of CM inductance is achieved where the CM inductance of a toroidal CM choke can be defined by [14]:

$$L_{CM} = A_L N^2 \frac{\mu'(f)}{|\bar{\mu}(f = 0\text{Hz})|} \quad [\text{H}], \quad (1)$$

Where N = number of turns,

A_L = inductance per turn,

$\bar{\mu}$ = complex permeability,

μ' = real part of complex permeability ($\bar{\mu}$).

On the other hand, as DM current passes through a CM choke, the mutual flux is completely canceled. However, there are leakage fluxes at each winding of a CM choke which can moderately suppress the DM current. The leakage inductance of a toroidal CM choke (DM inductance) can be approximated [12]:

$$L_{DM} = \mu_{DM_e} \frac{0.4\pi N^2 A_e}{l_e \sqrt{[(\theta/360) + (\sin(\theta/2)/\pi)]}} \quad [\text{H}], \quad (2)$$

where μ_{DM_e} = the effective permeability for leakage flux,

θ = winding angle,

A_e = effective cross-sectional area,

l_e = effective mean length of the core.

However, it should be note that the DM and CM inductances of a CM choke can be obtained easily by the measurements. Figs. 2 (a) – (b) show the measurement setup to measure the DM and CM inductances of a CM choke, respectively. By shorting one winding and measuring the leakage inductance at the other winding, the DM inductance can be achieved by divided the measured result by 2 since it is the summation of the leakage inductance of both windings. For CM inductance measurement of a CM choke, it can be obtained by using asymmetrical test circuit as shown in Fig. 2 (b) [15].

3. Proposed Magnetic Integration Technique of LCL Filters Used in Grid-Tied PV Power Systems for Conducted EMI Reduction

Traditionally, one inductor needs at least one set of magnetic core. Since a LCL filter proposed in this paper is composed of two CM chokes and two C_Y capacitors as shown in Fig. 3. As a result, a LCL filter needs at least two sets of UI (or EI) magnetic cores.

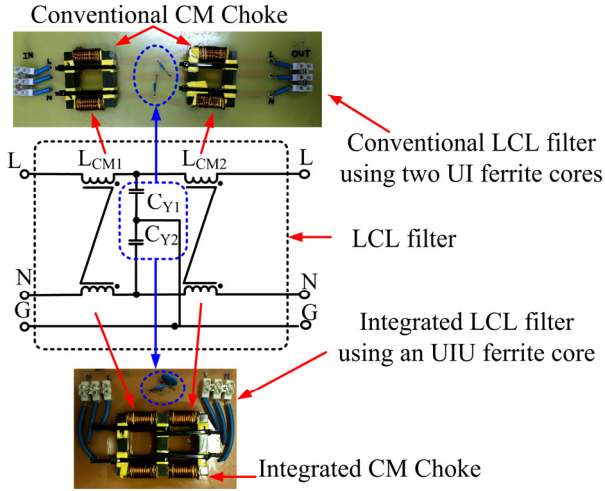


Fig. 3. Comparison of proposed integrated LCL filter with UIU magnetic core and a conventional LCL filter with two separated UI magnetic cores.

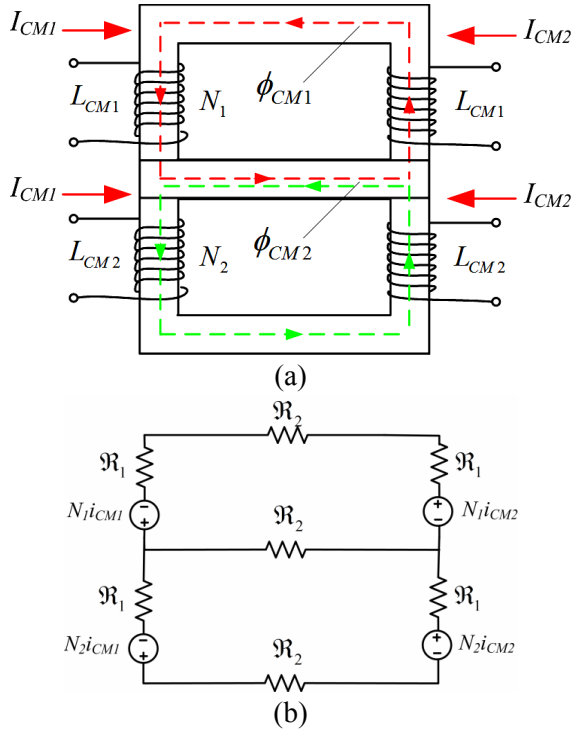


Fig. 4. Proposed Integrated CM chokes using UIU core; (a) winding configuration; (b) magnetic circuit derivation.

The purpose of this paper is to eliminate the use of magnetic parts as much as possible by not affecting the EMI reduction performance of the filters. Figs. 4-5 show the proposed UIU magnetic core (possible to use the EIE magnetic core as well) for a LCL filter instead of using two sets of UI magnetic cores. It can be seen that with the proposed technique one magnetic part ("I" core) can be eliminated [16-19].

Theoretically speaking, according to [16-19], since

the winding configurations of both CM chokes are symmetrically distributed on the outer legs of the two U-cores where the shared I-core provides a low-reluctance return path, the flux cancellation at the shared I-core could be obtained because CM currents passing through two CM chokes are in-phase. As shown in Fig. 4 (a), it can be seen that the directions of generated fluxes by CM chokes are cancelled each other at the shared I-core. It can be concluded that there is no dc flux existing in the shared I-core. The mutual fluxes produced by CM currents passing through CM chokes circulate only in the outer legs of the U cores. As a result, two CM chokes seem to decouple by shared I-core.

3.1. General Assumptions

In order to design a LCL filter optimally, the inductance approximation of proposed integrated magnetic circuit must be known. For sake of simplicity, the following assumptions must be defined to approximate the inductance values:

- All magnetic fluxes are decoupled completely;
- The leakage fluxes are not taken into account;
- The number of turns of CM chokes are equal to N .

With above assumptions, the inductances of CM chokes with proposed UIU magnetic core can be approximated.

3.2. Inductance Approximations of Proposed UIU Magnetic Core

Fig. 4 (a) shows UIU core with winding configuration in order to integrate two CM chokes of conventional LCL filter used in grid-tied PV power systems. Fig. 4 (a) can be converted into magnetic circuit as shown in Fig. 4 (b). With the defined assumptions, DM and CM inductances can be determined.

3.2.1 Approximation of CM Inductance

Since the number of turns of CM chokes is set to be equal ($N = N_1 = N_2$) and the CM current is equal to $I_{CM} = I_{CM1} + I_{CM2}$, thus the CM inductance can be determined by writing the KVL equations based on magnetic circuit as shown in Fig. 4 (b) as follows:

$$\begin{bmatrix} 2(\mathfrak{R}_1 + \mathfrak{R}_2) & -\mathfrak{R}_2 \\ -\mathfrak{R}_2 & 2(\mathfrak{R}_1 + \mathfrak{R}_2) \end{bmatrix} \begin{bmatrix} \phi_{CM1} \\ \phi_{CM2} \end{bmatrix} = \begin{bmatrix} NI_{CM} \\ NI_{CM} \end{bmatrix} \quad (3)$$

From Eq. (3), the CM inductance can be approximated as follows:

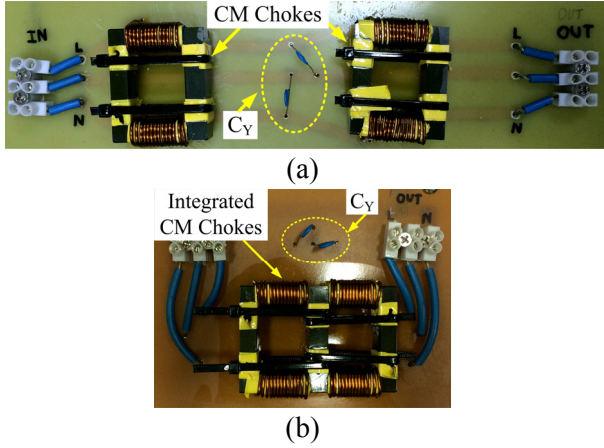


Fig. 5. LCL filter under test with: (a) conventional two separated CM chokes using two UI cores ($C_{Y1}=C_{Y2}=3.3\text{ nF}$) (b) proposed integrated CM chokes using a UIU core ($C_{Y1}=C_{Y2}=3.3\text{ nF}$).

$$L_{CM} = N^2 \frac{2(\mathfrak{R}_1 + \mathfrak{R}_2) + \mathfrak{R}_2}{4(\mathfrak{R}_1 + \mathfrak{R}_2)^2 - \mathfrak{R}_2^2} [\text{H}], \quad (4)$$

where \mathfrak{R}_1 and \mathfrak{R}_2 are magnetic reluctances of magnetic circuit as shown in Fig. 4 (b).

3.2.2 Approximation of DM Inductance

In order to simplify the equation to determine the DM inductance value of proposed integrated magnetic circuit, the winding arrangement of N_1 and N_2 are assumed to be wound on the same leg.

Using the approximation method by [20], the leakage inductance of each CM choke, which acts as a DM inductance, can be predicted by:

$$L_{DM} = \frac{4\pi(MLT)N^2}{a} \left(c + \frac{b_1 + b_2}{3} \right) [\text{nH}], \quad (5)$$

where MLT = mean length turn [cm],
 a = winding length [cm],
 b_1 = winding build of N_1 [cm],
 b_2 = winding build of N_2 [cm],
 c = thickness of insulation between N_1 and N_2 [cm].

3.2.3 Insertion Loss of proposed LCL Filter

Theoretically, a LCL filter provides the insertion loss at rate of 60 dB/decade above the cutoff frequency (f_c), and this type of filter is suitable for low source (Z_s) and load impedances (Z_L).

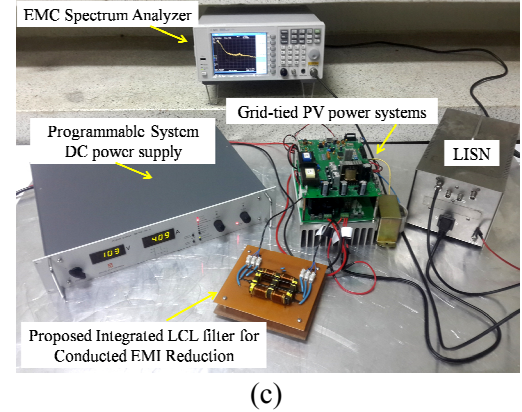
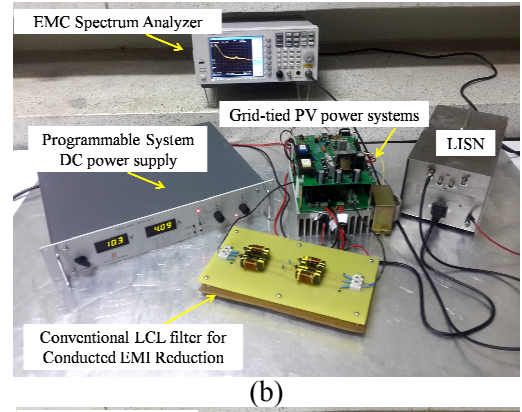
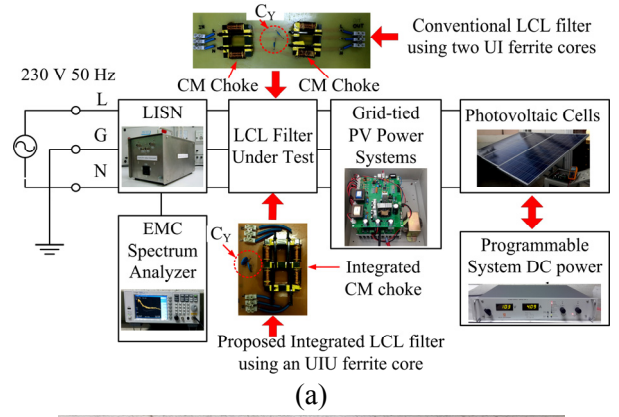


Fig. 6. The EMI measurement setup: (a) testing block diagram; (b) conventional LCL filter using two separated UI ferrite cores; (c) proposed integrated LCL filter using an UIU ferrite core.

Generally, LCL filter normally sets $L_{CM} = L_{CM1} = L_{CM2}$. The insertion loss of proposed LCL filter can be determined by [21]:

$$IL = 20 \log \left(1 + j\omega \left(\frac{2L_{CM}}{Z_s + Z_L} + C_{YT} \frac{Z_s Z_L}{Z_s + Z_L} \right) - \omega^2 C_{YT} L_{CM} - j\omega^3 \left(\frac{C_{YT} L_{CM}^2}{Z_s + Z_L} \right) \right) [\text{dB}], \quad (6)$$

where

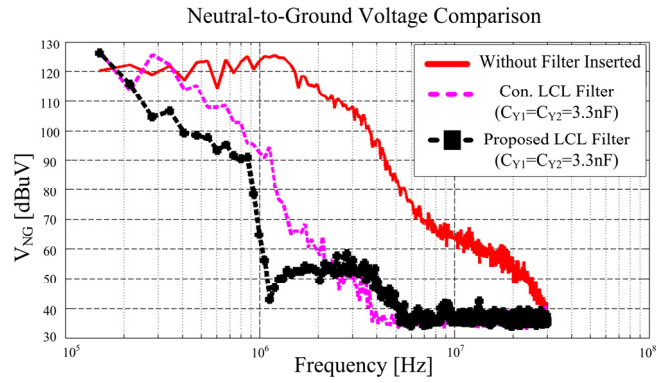
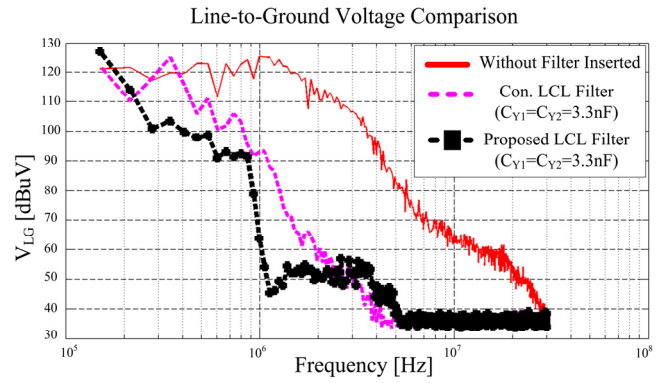
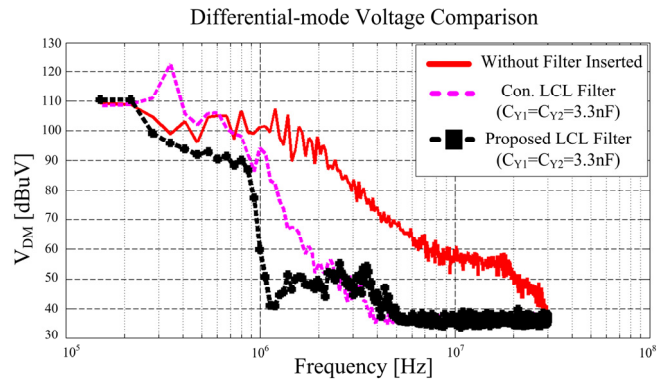
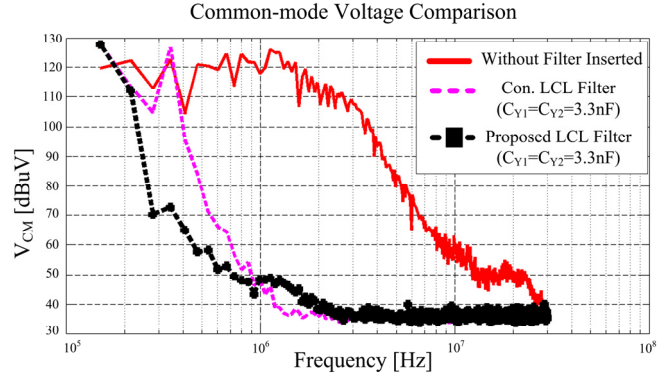


Fig. 7. The comparisons of measured EMI of the LCL filter with proposed UIU magnetic core and with two separated UI magnetic cores: (a) CM; (b) DM; (c) line-to-ground; (d) neutral-to-ground.

$$f_c = \frac{1}{2\pi \left(\frac{2L_{CM}}{Z_S + Z_L} + C_{YT} \frac{Z_S Z_L}{Z_S + Z_L} \right)} \quad [\text{Hz}],$$

$$C_{YT} = C_{Y1} + C_{Y2} \quad [\text{F}].$$

It should be noted that Eq. (6) is not only derived for EMI filter designers, but it shows the effects of load and source impedances on the EMI reduction performance of a LCL filter also. By using Eq. (6) and the procedure provided in [22], the LCL filter can be optimally designed.

4. Experimental Validations and Discussions

Since the proposed integrated LCL filter is designed for being used in grid-tied PV power systems in order to limit conducted EMI (especially CM emission) generated by them, for this reason, the following experiments are carried out in order to guarantee that the proposed integrated LCL filter can be used without any degradation of EMI reduction performance comparing to a conventional one. The testing block diagram of the experiments shows in Fig. 6 (a). The EMI reduction performances of a conventional LCL filter and the proposed integrated LCL filter are evaluated and compared where the measurement setups are shown in Figs. 6 (b) and (c), respectively.

The grid-tied PV power system is designed to inject the power to the grid utility at the rated power up to 750 W, and it is the cascade of PV connected to boost converter and then to full-bridge inverter where the system is controlled by the microcontroller (dsPIC30F6010A). However, because of the limitations of the measurements, in these tests, the injected power to the grid utility is at the rate of 500 W via the line impedance stabilization network (LISN) which includes the CM and DM noise separator network [23] as shown in Fig. 6. Moreover, for EMI measurement test, the PV is replaced by programmable system DC power supply (Delta Elektronika: SM 400-AR-8). According to CISPR 22 standard, the conducted EMI is measured through the EMC spectrum analyzer (Agilent Spectrum Analyzer: N9320B) with the frequency range of interest starting from 150 kHz up to 30 MHz and BW at 9 kHz.

For comparison purposes, all implementations were made with the conditions that (a) all magnetic parts use EI-50 core size; (b) in all cases, the number of turns is equal to 14 and (c) two CY equal to 3.3 nF (mica capacitors) are used. The EMI reduction performances among grid-tied PV power systems without any filter inserted, with traditional separated magnetic cores, and with proposed integrated magnetic core using UIU core are evaluated and compared as shown in Figs. 7 (a) - (d) for EMI comparisons in terms of CM, DM, line-to-ground, and neutral-to-ground, respectively.

From Fig. 7 (a), it shows that the CM reduction performance of proposed integrated LCL filter using UIU core does not only suppress the CM noise over the conducted EMI frequency range, but it also provides higher insertion loss up to about 70 dBuV comparing to the case of without filter inserted. By comparing to the case of with conventional filter inserted, the proposed filter provides higher insertion loss up to about 50 dBuV over the frequency range 200 kHz - 1 MHz. However, at the frequency range of 1 MHz - 30 MHz, it provides the similar results.

Fig. 7 (b) shows the comparison of DM reduction performance among the case of without any filter inserted, proposed integrated LCL filter using UIU core, and a conventional LCL filter using separated magnetic cores. It can be seen that both conventional and proposed LCL filter can slightly suppress the DM noise due to its leakage inductance. By comparing between conventional and proposed LCL filter, the proposed LCL filter provides higher insertion loss up to about 50 dBuV over the frequency range of 200 kHz - 2 MHz. However, at the frequency range of 2 MHz - 30 MHz, it provides the similar results.

Figs. 7 (c) - (d) compare the EMI measured results (line-to-ground and neutral-to-ground) of the cases of without filter inserted, with conventional LCL filter and with proposed integrated LCL filter. Obviously, the proposed integrated LCL filter using UIU core provides higher insertion loss up to about 40 dBuV at frequency range from 200 kHz - 2 MHz, comparing to a conventional LCL filter. However, at the frequency range from 2 MHz up to 30 MHz, the good agreement between conventional and proposed LCL filters is achieved.

5. Conclusion

The approach to integrated magnetic core parts of a conventional LCL filter is proposed in this paper. With the proposed magnetic core shape and winding configuration, two sets of UI magnetic cores of a conventional LCL filter can be integrated into one set of an UIU magnetic core that means one magnetic part ("I" core) can be eliminated. To assure the EMI reduction performance of proposed concept, the conducted EMI measurements (in terms of CM, DM, line-to-ground, and neutral-to-ground) in case of the grid-tied PV system without any filter inserted, with conventional separated magnetic cores, and with proposed integrated magnetic core of LCL filter are evaluated and compared. According to the experimental results, it can be summarized that the proposed integrated LCL filter provides higher insertion loss comparing to a conventional one up to about 50 dBuV over the frequency range of 200 kHz - 2 MHz. However, at the frequency range of 2 MHz - 30 MHz, there is no different between proposed filter and conventional filter. By using the proposed magnetic core shape with winding configuration, the

improvement of total magnetic volume, total magnetic cost, and core losses could be achieved without degradation of its EMI reduction performance. However, it should be noted that this paper proposes a technique to integrate EMI filter's inductors, but it might also be applied to harmonic filter design as well.

6. Acknowledgments

This work was supported by the research grant from Srinakharinwirot University (242/2556). Author would like to thank Mr. Sirimongkhon Phongthongcharoen, Mr. Wachira Pongkasetsilp, Mr. Apisak Meerat, Mr. Sathaporn Uraiphan and Ms. Siriporn Sirawuttinanon for the experimental demonstrations.

References

1. B. K. Bose, "Global Energy Scenario and Impact of Power Electronics in 21st Century," *IEEE Trans. Ind. Electron.*, vol. 60, no. 7, pp. 2638–2650, Jul 2013.
2. M. Liserre, T. Sauter and J.Y. Hung, "Future Energy Systems: Integrating Renewable Energy Sources into the Smart Power Grid Through Industrial Electronics," *IEEE Industrial Electronics Magazine*, vol. 4, no. 1, pp. 18–37, March 2010.
3. J. M. Carrasco, L.G. Franquelo, J.T. Bialasiewicz, and et.al., "Power-Electronic Systems for the Grid Integration of Renewable Energy Sources: A Survey," *IEEE Trans. Ind. Electron.*, vol. 53, no. 4, pp. 1002–1016, June 2006.
4. S. B. Kjaer, J.K. Pedersen and F. Blaabjerg, "A Review of Single-phase Grid-tied Inverters for Photovoltaic Modules," *IEEE Trans. Ind. Appl.*, vol. 41, no. 5, pp. 1292–1306, Sep/Oct 2005.
5. V. Tarateeraseth, "Systematic Power Line EMI Filter Design for SMPS, Part I: Common-mode and Differential-mode Conducted EMI Generation Mechanisms," *IEEE EMC Society Newsletters*, vol. 231, Fall 2011. Available: <http://ewh.ieee.org/soc/emcs/newsletters.html>
6. R. Araneo, S. Lammens, M. Grossi and S. Bertone, "EMC Issues in High-Power Grid-tied Photovoltaic Plants," *IEEE Trans. Electromagn. Compat.*, vol. 51, no. 3, pp. 639–648, Aug 2009.
7. W. Weimin, S. Yunjie, L. Zhe, and et.al., "A Modified LLCL Filter With the Reduced Conducted EMI Noise," *IEEE Trans. Power Electron.*, vol. 29, no. 7, pp. 3393–3402, July 2014.
8. V. Tarateeraseth, "EMI filter design: Part III: Selection of filter topology for optimal performance," *IEEE Electromagn. Compat. Mag.*, Second Quarter 2012, pp. 60–73.
9. Rixin Lai, Y. Maillet, F. Wang, and et.al., "An Integrated EMI Choke for Differential-mode and Common-mode Noise Suppression," *IEEE Trans. Power Electron.*, vol. 25, no. 3, pp. 539 – 544, March 2010.
10. J. Biela, A. Wirthmueller, R. Waespe, and et.al., "Passive and Active Hybrid Integrated EMI Filters," *IEEE Trans. Power Electron.*, vol. 24, no. 5, pp. 1340 – 1349, May 2009.
11. F. Luo, D. Boroyevich, P. Mattevelli, and et.al., "An Integrated Common Mode and Differential Mode Choke for EMI Suppression Using Magnetic Epoxy Mixture," in *2011 Proc. IEEE Applied Power Electron. Conf. and Expo.*, pp.1715–1720.
12. W. Tan, C. Cuellar, X. Margueron and N. Idir, "A Common-Mode Choke Using Toroid-EQ Mixed Structure," *IEEE Trans. Power Electron.*, vol. 28, no. 1, pp. 31–35, Jan 2013.
13. X. Wu, D. Xu, Z. Wen, and et.al., "Design, Modeling, and Improvement of Integrated EMI Filter with Flexible Multilayer Foils," *IEEE Trans. Power Electron.*, vol. 26, no. 5, pp.1344 –1354 2011.
14. M.L. Heldwein, L. Dalessandro and J.W. Kolar, "The Three-Phase Common-Mode Inductor: Modeling and Design Issues," *IEEE Trans. Ind. Electron.*, vol. 58, no. 8, pp. 3264–3274, Aug 2011.
15. K. Kostov and J. Kyyrä, "Common-mode Choke Coils Characterization," *13th European Conference on Power Electronics and Applications (EPE 2009)*, pp.1-9, 8-10 September 2009.
16. V. Tarateeraseth, "An Integrated Magnetic Circuit for Differential-mode and Common-mode Chokes of EMI Filters," *ECTI Transactions on Electrical Engineering, Electronics, and Communications (ECTI-EEC)*, Vol 12, No 1, February 2014.
17. Z. Ouyang, Z. Zhang, O. C. Thomsen and M. A. E. Andersen, "Planar Integrated Magnetics (PIM) Module in Hybrid Bidirectional DC-DC Converter for Fuel Cell Application," *IEEE Trans. Power Electron.*, vol. 26, no. 11, pp.3254 –3264, 2011.
18. Z. Ouyang; G. Sen, O.C. Thomsen, M.A.E. Andersen, "Analysis and Design of Fully Integrated Planar Magnetics for Primary–Parallel Isolated Boost Converter," *IEEE Trans. Ind. Electron.*, vol. 60, no.2, pp. 494-508, Feb 2013.
19. D. Pan, X. Ruan, C. Bao, and et.al., "Magnetic Integration of the LLC Filter in Grid-Connected Inverters," *IEEE Trans. Power Electron.*, vol. 29, no. 4, pp. 1573 –1578, April 2014.
20. Colonel Wm. T. Mclyman, *Transformer and Inductor Design Handbook*, 3rd edition, Marcel Dekker Inc., p. 17-5, 2004.
21. Kenneth L. Kaiser, *Handbook of Electromagnetic Compatibility*, 1st edition, CRC Press, ch. 7, 2004.
22. V. Tarateeraseth, K. Y. See, F. Canavero and R.W.Y. Chang, "Systematic electromagnetic interference filter design based on information from in-circuit impedance measurement," *IEEE Trans. Electromagn. Compat.*, vol. 52, no. 3, pp. 588–598, Aug 2010.
23. D. Sakulhirak, V. Tarateeraseth, W. Khan-ngern, and N. Yoothanom, "A new simultaneous conducted electromagnetic interference measuring and testing device," *The 19th International Zurich Symposium On Electromagnetic Compatibility*, APEMC 2008, 19-23 May 2008.